# DWPT-Integrated Microscopic Traffic Flow for Distribution Grid Voltage Stability Analysis

Travis Newbolt, Student Member, IEEE, Paras Mandal, Senior Member, IEEE, Hongjie Wang, Senior Member, IEEE, and Regan Zane, Senior Member, IEEE

Abstract—This paper examines an application of a two-lane microscopic Traffic Flow (TF) simulation to comprehend the impact of the complex behavior of Dynamic Wireless Power Transfer (DWPT) charging systems onto electric power distribution grids. The proposed approach utilizes real-world data to determine a more accurate TF density at each time interval. The simulation is carried out considering all vehicles, whether electric vehicles (EVs) or non-electric, and they have a randomized lane changing behavior and fluctuating velocities following a leading car model. Three different scenarios are conducted for 5 mile, 10 mile, and 15 mile DWPT networks that are proportionally connected to an IEEE 33-bus distribution grid. Our findings indicate that EVs' average State-of-Charge (SOC) increases proportionally and significantly at each DWPT network length. Furthermore, the load demand generated from the DWPT network also increases proportionally with its length; and this increment in load demand causes adverse impacts on distribution grid voltage magnitudes exceeding operational standards that leads to equipment failure or blackout events.

Index Terms—Dynamic wireless power transfer, electrified transportation, EV charging, grid stability, microscopic traffic flow.

## I. INTRODUCTION

The transition of transportation infrastructures to an electrified apparatus is one of the many challenges while integrating electric vehicles (EVs) into power distribution grids. As the penetration of EVs into transportation networks increases, the necessary charging energy from distribution systems can be reasonably assumed to fluctuate proportionally. This growth, although it will alleviate charging anxiety, improve air quality, and reduce annual carbon emissions, it will also require tremendous efforts to ensure electric power distribution systems can withstand the added load demand [1]–[3]. According to [4], the U.S. would need to produce approximately 20%-50% more energy to sustain an all EV fleet within transportation infrastructures. This increase in load demand will potentially require, in certain locations, the modification

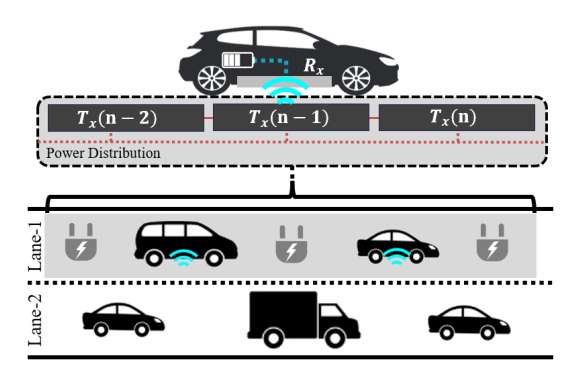


Fig. 1. Microscopic traffic flow topology of a two-lane highway infrastructure with a single DWPT charging lane.  $\triangleright$  *Lane-1:* is the charging lane consisting of numerous Transmitter (Tx) pads that transfer energy to EVs through a Receiver (Rx) pad.  $\triangleright$  *Lane-2:* is a non-charging lane for all vehicles.

and/or modernization of distribution grid equipment (i.e., distribution lines, transformers, etc.) to facilitate EV charging even though localized Renewable Energy Sources (RES), such as photovoltaics and wind turbines, are capable of mitigating a portion of the overall load demand. Furthermore, innovative methods to mitigate or lessen the burden of EV charging are necessary to allow individuals to actively utilize their vehicles without restricting access to energy.

In recent years, a new approach in EV charging has been proposed that can allow EVs to traverse through transportation networks while charging. Fig. 1 illustrates an evolving EV in-motion charging system, which is generally known as Dynamic Wireless Power Transfer (DWPT). This type of charging system is predominately implemented with consecutively embedded inductive coils known as Transmitter (Tx) pads within the pavement of transportation networks and a Receiver (Rx) pad that is installed below the chassis of an EV [5]–[8]. One of the many challenges associated with DWPT is the scalability to large-scale systems where hundreds of Tx pads are implemented to produce relatively long lasting charging access while the vehicle is traversing at highway speeds. The majority of research, in the context of DWPT systems, are implemented at small-scale where only one to four Tx pads are analyzed at the same time. Zakerian et al. [9] utilized a single Tx pad to develop a frequency and voltage tracking regulation model to improve the overall efficiency of the DWPT system to approximately 72%. In [10], the authors implemented a four Tx pad system in connection with artificial neural networks to predict the power output of DWPT systems

This work is based in part upon work supported by the National Science Foundation (NSF) through the ASPIRE Engineering Research Center under Award# 1941524 and CAREER Award# 2239169, and the Department of Energy/ National Nuclear Security Administration under Award# DE-NA0004016.

T. Newbolt and P. Mandal are with the Power and Renewable Energy Systems (PRES) Lab., Department of Electrical and Computer Engineering, The University of Texas at El Paso, TX 79968, USA (e-mail: tmnewbolt@miners.utep.edu; pmandal@utep.edu).

H. Wang and R. Zane are with the Department of Electrical and Computer Engineering, Utah State University, Logan, UT 84341 USA (e-mail: hongjie.wang@usu.edu; regan.zane@usu.edu).

with an accuracy of about 87%. Varghese *et al.* [11] simulated a three Tx pad system to analyze a multi-receiver pad approach to simplify the adoption of various duty classes of EVs in DWPT charging infrastructures. Liu *et al.* [12] considered multiple Rx pads across a single Tx pad with a voltage doubler rectifier to develop a novel approach in mitigating output voltage fluctuations. Xue *et al.* [13] validated a design for a 120 kW charging system where a single Tx pad was implemented in simulations.

These approaches are commonly implemented in simulation software such as PLECS, Ansys Maxwell, and MATLAB Simulink. However, the computational burden for these approaches is typically high as the time-scale of the simulations ranges from nanoseconds to milliseconds. For the purposes of distribution grid analysis with the incorporation of largescale DWPT networks, these time-scales are not adequate as the processing time would be too large. In our previous work [14], a novel approach for reducing the computational burden of DWPT networks is utilized to determine the load demand profile for a single-lane large-scale DWPT network with numerous EVs traversing the system over a period of a week. Although the results presented in [14] are sufficient in generating the load demand profiles for distribution grid analysis, the modeling of the behavior of individual EVs traversing through the system can be improved further to track/mimic free-flowing Traffic Flow (TF) that can provide for a more accurate load demand profile when multiple lanes are considered, as depicted in Fig. 1. Hence, in contrast to the existing literature, this paper significantly contributes to the field of evolving electrified-transportation networks, thus the major contributions of this paper are the following: (1) Development of a microscopic TF algorithm for a two-lane DWPT network that enhances stability analysis of distribution grids, (2) Demonstration and analysis of DWPT load demand profiles at large-scale, (3) Impact analysis of large-scale DWPT networks in distribution grid to ascertain the diverse effects caused by EV in-motion charging, and (4) Development of a computationally efficient method that can provide insights to the power system operations about EV in-motion charging infrastructure.

This paper is organized as follows. Section II presents the proposed approach to develop the two-lane microscopic TF simulation. Sections III and IV present the simulations/data setup and analysis of DWPT network and impact on grid. Section V concludes with the major findings of the paper.

## II. PROPOSED APPROACH

This section describes the development of the proposed method to generate DWPT load demands utilizing a two-lane microscopic simulation that incorporates numerous EVs, different duty classes, fluctuating velocities, and randomized lane-changing behavior.

# A. Background of Microscopic Simulation

In transportation engineering, the study of vehicle behavior through roadway networks that mimic real-world driving patterns is utilized to analyze the structural integrity of roadway networks, construction methods to reduce congestion, planning operations, and maintenance scheduling. Simulations of TF for varying types of roadway networks can be divided into two separate categories: macroscopic and microscopic [15]. Macroscopic simulations analyze the entirety of the TF, while microscopic simulations observe the individual behaviors of each vehicle. For the purposes of this paper, the focus will be microscopic simulations where the model attempts to analyze individual driving behavior in relation to other vehicles on the roadway system [16]. In this paper, a microscopic simulation of a two-lane highway is constructed that accounts for the individual driving behavior of EVs and non-EVs. A typical approach of microscopic simulations is developed to incorporate lane-changing behavior through randomized processes and carfollowing models that fluctuate vehicle velocities according to the proximity to leading or adjacent vehicles in the roadway network. In this paper, to ensure that the TF simulation does not allow vehicles to overlap one another while traversing through the network, the positional data of each vehicle is tracked by

$$x = (x_{\alpha} - l_{\alpha}) + x_o \quad , \tag{1}$$

where x is the gap distance,  $x_{\alpha}$  is the position of the leading vehicle,  $l_{\alpha}$  is the leading car length, and  $x_{o}$  is the position of the currently observed vehicle. Furthermore, the gap distance is utilized to fluctuate the velocity of each vehicle, which is given by

$$X(t) = \begin{cases} +v(t), & \text{if } x > \gamma \\ -v(t), & \text{otherwise} \end{cases}$$
, (2)

where  $\gamma$  is the minimum distance between the leading and currently observed vehicle, v(t) is the velocity, and X(t) is the finalized positional data for the next time interval. Then the TF simulation is updated multiple times at each time step to track the movements of each vehicle by implementing

$$X_f(t) = F(X(t), Y(t), l_o, v(t))$$
 , (3)

where X(t) is the updated positional data, Y(t) is the lane of travel,  $l_o$  is the length of the vehicle, and v(t) is the velocity of the vehicle.

## B. Microscopic TF Algorithm for DWPT Network

Fig. 1 demonstrates the proposed roadway network where Lane-1 represents the DWPT charging system (e.g., gray highlighted area) and all vehicles (non-charging) is represented by Lane-2. The network is constructed as an array that contains 2-by-N indices, where N is the length of the overall transportation infrastructure. This method is different from our previous approach [14] by not restricting the behavior of vehicles to a singular lane of travel. Fig. 2 presents the step-by-step processes of the proposed microscopic algorithm that incorporates the calculation of the DWPT load demand. In Step 1, the input and initialization process utilizes object-oriented programming to store and collect vehicle specifications during the TF simulation. Each vehicle object has two constructors that are utilized to gather information to calculate

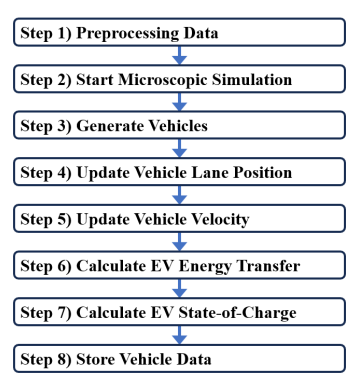


Fig. 2. Flowchart of microscopic traffic flow simulation for DWPT network.

the overall behavior of each vehicle type during each time step. Our another previous work [17], presents a Monte Carlo algorithm to convert historical hourly TF into secondly time intervals which is utilized in this paper to generate the initial time entry for each vehicle in the simulation. Additionally, the dimensional characteristics of the DWPT network are determined by taking into account the Rx pad limits. Tx pad limits, length of Tx pads, length of the Rx pad, gap distance between each Tx pad, lane drifting percentages, and length of overall DWPT as demonstrated in [14].

After the initialization process has concluded, the microscopic simulation begins by determining how many vehicles are actively traversing the network at each time step. This process is performed to reduce the computational burden when the number of vehicle objects is large. Then each active vehicle is generated in the network according to their individual time of entry at Step 3. In this paper, it assumed that all vehicles will enter the network at a randomized lane regardless if the vehicle is an EV or not. However, if two vehicles have the same time of entry and starting lane, then one vehicle will be modified to start on the other lane to avoid overlapping. Steps 4 through 5 are where each vehicles positional data and velocities are updated within the simulation. In this paper, two different lane changing behaviors are implemented to differentiate between EVs and non-EVs and are defined as:

$$\begin{split} Y_{none}(t) &= \begin{cases} L(-y), & \text{if } P=1, \ x \leq \gamma, \ \text{and} \ y_{\alpha} \leq \gamma_{o} \\ L(y), & \text{otherwise} \end{cases}, \quad \text{(4)} \\ Y_{EV}(t) &= \begin{cases} L(-y), & \text{if } P=1, \ L_{o}=2, \ \text{and} \ y_{\alpha} \leq \gamma_{o} \\ L(y), & \text{otherwise} \end{cases}, \quad \text{(5)} \end{split}$$

$$Y_{EV}(t) = \begin{cases} L(-y), & \text{if } P = 1, \ L_o = 2, \text{ and } y_\alpha \le \gamma_o \\ L(y), & \text{otherwise} \end{cases}$$
, (5)

where P is the probability for the vehicle to choose to change lanes,  $y_{\alpha}$  is a check to ensure that no vehicles are within the minimum gap distance  $\gamma_o$  for the opposite lane, and  $L_o$  is the initial lane of travel. For EVs, it is assumed that they prioritize the need to be on the DWPT charging lane and will seek to remain/change to it regardless of congestion. The behavior of non-EVs is assumed to have no prioritization towards charging. Instead non-EVs will prioritize speed of travel to avoid any congestion that is produced in the TF simulation.

The final process illustrated in Fig. 2 is to calculate energy transferred and the State-of-Charge (SOC) for all EVs that are actively traversing the DWPT network. The calculation is performed utilizing an algorithm presented in Section III of [17], where the specifications of each EV is implemented to determine a new SOC and load demand profile at each time step. In addition to the algorithm, the modification demonstrated in Section II of [14] is implemented to increase the accuracy of the calculated load demand by utilizing a novel convolutional approach.

#### III. DATA DESCRIPTION AND SIMULATION SETUP

This section presents the data utilized to simulate numerous vehicles traversing through a DWPT network simulation with a purpose to demonstrate how each dataset is implemented at the preprocessing stage to generate the microscopic simulation.

# A. Traffic Flow Data Description

The TF density of vehicles that enter into the network is determined by historical data collected for the Interstate-10 highway in El Paso, Texas region for 2021 [18]. This data is condensed to the averaged seasonal TF for each day of the week at intervals of an hour. In this paper, the traffic flow for a typical Monday during the fall season is implemented for a 24hour period at intervals of seconds. Fig. 3(a) illustrates the total number of vehicles entering into the DWPT network and how many of them are classified as EVs (i.e., the solid red line), which equates to 25% of the TF for each hour. This data is then converted into secondly TF using the Monte Carlo process that we formulated on our previous work [14]. In Fig. 3(b), each vehicles initial lane of entry is illustrated, where the numbering is determined by random processes where Lane-1 had a 60% probability and Lane-2 had a 40%.

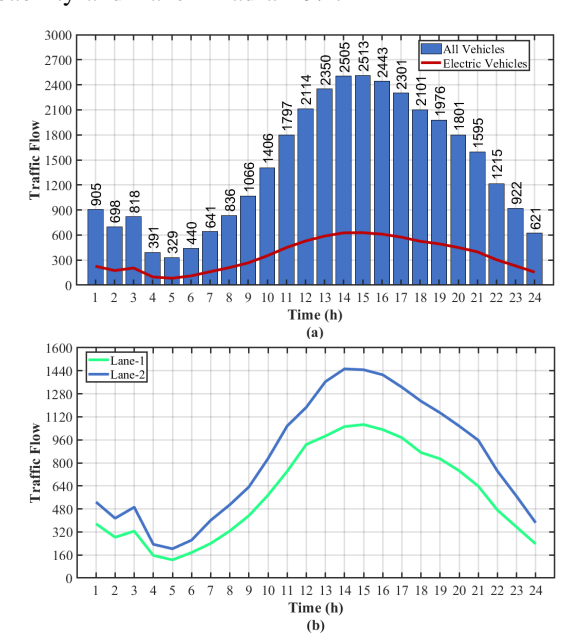


Fig. 3. Traffic flow totals. (a) All vehicle types and electric vehicles, and (b) All vehicle types on Lane-1 and Lane-2 of DWPT network.

## B. Vehicle Specification Description

For a real-world scenario of free flowing TF on a highway network, there needs to be various types of vehicles within

TABLE I LIGHT-DUTY EV SPECIFICATIONS

Specifications	L1	L2	L3	L4	L5	L6
Capacity (kWh)	53.6	60	40	64	64	42.2
Mass (Mg)	1.61	1.62	1.55	1.68	1.74	1.34
Length (m)	4.69	4.16	4.48	4.18	4.37	4.01
Cross Sect. Area (m)	2.16	2.28	2.26	2.29	2.30	2.30
Drag Coefficient	0.23	0.31	0.28	0.29	0.29	0.29
Charging Capacity (kW)	170	80	50	100	100	50

L1: Tesla Model 3, L2: Chevy Bolt, L3: Nissan Leaf, L4: Hyundai Kona, L5: Kia e-Niro, L6: BMW i3

TABLE II
MEDIUM AND HEAVY-DUTY EV SPECIFICATIONS

Specifications	M1	M2	M3	H4
Capacity (kWh)	112	131	200	564
Mass (Mg)	2.65	2.61	2.81	11.1
Length (m)	4.95	5.91	5.69	21.3
Cross Sect. Area (m)	2.70	3.80	3.74	11.6
Drag Coefficient	0.25	0.40	0.30	0.70
Charging Capacity (kW)	195	150	250	350

M1: BMW iX, M2: Ford F-150 Lightning, M3: Cadillac Escalade IQ, H1: Volvo VNR Electric 4x2 Tractor

the simulation to have an accurate model. In this paper, six different Light-Duty Vehicles (LDVs), three Medium-Duty Vehicles (MDVs), and one Heavy-Duty Vehicle (HDV) are implemented. Each of these models are based on the most popular EVs on the market (i.e., LDV and MDV models) or estimated specifications (i.e., HDV). Table I and II present the specifications for each vehicle type implemented in the microscopic simulation including the vehicles type considered in this paper [19]. Each of these specifications are utilized to calculate the behavior of the vehicle while in-motion, and in the case of an EV, they are essential to determine the SOC, energy discharged, and/or energy transferred through the DWPT network. In this paper, each EV is restricted from charging past 80% SOC to limit the number of EVs that are actively utilizing the network to those vehicles that have a higher priority to charge [20]. Furthermore, each vehicle type is considered to have a different density probability in the TF simulation according to the U.S. Department of Transportation statistics where LDVs, MDVs, and HDVs will have 73.6%, 22.5%, and 3.9% respectively [21]. For each instances of a vehicle, the initial velocity and SOC is randomly selected uniformly from 45 mph-90 mph and 10%-90%, respectively.

# C. DWPT Network and Grid Connection Description

In this paper, three different lengths of DWPT networks of 5 miles, 10 miles, and 15 miles are implemented to investigate the impacts of large-scale DWPT networks onto a distribution grid. Each length constitutes a different scenario and interconnection within the grid. In Fig. 4, the topology of an IEEE 33-Bus distribution grid is illustrated to present how the DWPT network is attached. Each scenario will increase the number of buses that are attached to the DWPT network proportionally, where bus-6 through bus-8 will facilitate 5 miles of the charging system individually. Thus, for Scenario 1, only bus-6 is considered to be in connection with the DWPT network, whereas, Scenario 2 has bus-6 and bus-7 attached and the Scenario 3 utilizes all three buses 6–8. The characteristics of the DWPT network is designed to accommodate the largest

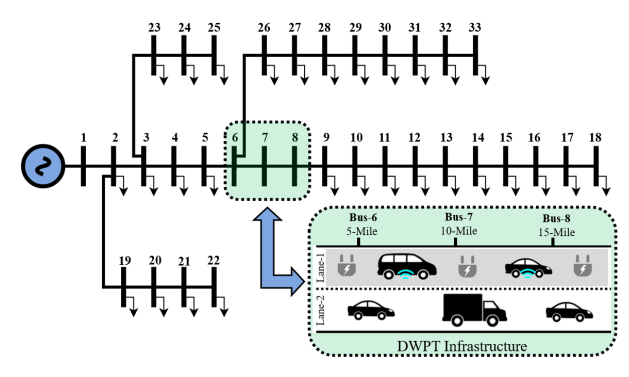


Fig. 4. Distribution grid topology for an interconnection of DWPT infrastructure at 5 mile incremental lengths.

charging capacity as presented in Table II. Therefore, the Tx pads charging capacity is 350 kW and the length and width is 3 m by 1 m, respectively. Additionally, the gap distance between each of the Tx pads are set to 0.025 m to produce a steady flow of energy through the system when the EV is traversing. The dimensional specifications for the DWPT network results in approximately 532 Tx pads per mile.

### IV. SIMULATION RESULTS AND DISCUSSION

This section presents the results for the two-lane microscopic TF simulations for varying lengths of DWPT networks. All simulations are conducted and obtained utilizing MATLAB version R2021b and MATPOWER version 7.

## A. Microscopic Traffic Flow Simulation Results

This paper focuses on developing a two-lane microscopic simulation to analyze DWPT networks in distribution grids. The results of the load demands generated by each of the three scenarios is presented in Fig. 5 where it can be seen that as the length of the network increases the magnitude of the

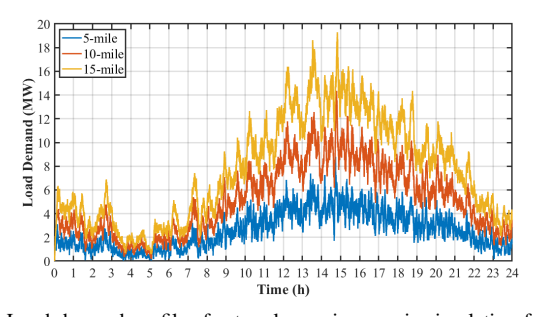


Fig. 5. Load demand profiles for two-lane microscopic simulation for 5, 10, and 15 mile DWPT transportation network.

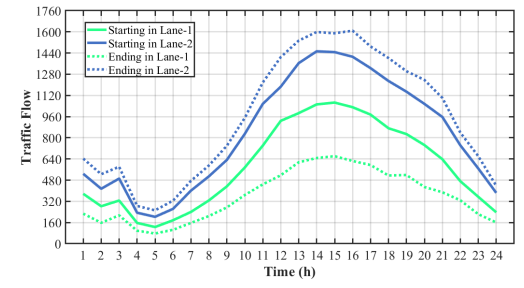


Fig. 6. Number of vehicles on each lane at the beginning and end of microscopic TF simulation.

load expands proportionally. This results can be expected since each EV will traverse through the network for longer periods of time as the length increases. Fig. 5 also demonstrates that the load demand between the hours of 8am and 11pm follow the TF pattern and drastically increases the slope of the load when the length of the network goes from 5 miles to 15 miles. Additionally, the load demand in Fig. 5 also fluctuates rapidly with the largest gap occurring in the 15 mile simulation where the maximum demand is approximately 18 MW during hour 13 and then suddenly drops to approximately 10 MW by hour 14. The rapid drop of approximately 8 MW of load can potentially have negative effects onto distribution grids if proper planning is not conducted.

Fig. 6 illustrates the change in the number of vehicles in each lane at the start and end of the simulation where Lane-2 increased the total number of vehicles traversing through the lane while Lane-1 had a decrease. This result is to be expected since only 25% of the TF is representative of the overall number of vehicles entering the roadway. Therefore, non-EVs that where assigned to Lane-1 initially would change lanes according to congestion rates more frequently.

In Figs. 7(a) through (c) the SOC for all EVs that traversed through the DWPT networks are compared to determine at which DWPT length the average user would benefit more considerably. Each of the sub-figures illustrates the maximum, minimum, averaged (i.e., the trend line), and all SOC for each EV. Fig. 7(a) presents the results of the 5 mile network with

Trend Line of Charge 150 50 75 100 250 Time (s) 80.0 All SOC Lin 75.0 Max Lin 70.0 Trend Lin 8 65.0 <del>වී</del> 60.0 55 ( 50.0 45.0 40.0 222 111 259 444 Time (s) 80.0 All SOC Line 75.0 Max Line ₹ 70.0 Trend Lin 8 65.0 0.00 Par 55.0 50.0 159 424 106 212 265 318 Time (s)

Fig. 7. State-of-charge for all EVs. (a) 5 mile DWPT length, (b) 10 mile DWPT length, and (c) 15 mile DWPT length.

an average increase in SOC of approximately 6%. Fig. 7(b) illustrates the results for the 10 mile simulation and produced an average increase of SOC of approximately 11%. Fig. 7(c) generated the highest increase of approximately 15% for the 15 mile DWPT network. This result is also expected because as the length of the DWPT network increases each EV will have more time to actively charge, which also translates to more load demand generated as seen in Fig. 5.

### B. Results for Voltage Stability Analysis of Distribution Grids

The results of the IEEE 33-bus distribution grid are presented in Fig. 8 where the voltage fluctuations at bus-6 through bus-8 are illustrated for each of the DWPT network lengths. In each sub-figure the threshold to determine whether the system has reached a voltage drop significant enough to cause severe damage to installed equipment or outage is classified as a decrease of -10% from the nominal [22]. The voltage profiles in Figs. 8(a) through (c) are similar in fluctuation with the only difference in the magnitude of drop as the bus number increases. For instance, bus-8 experiences a maximum drop during the 15 mile simulation of approximately 0.33 pu while bus-7 and bus-6 have a drop of approximately 0.28 pu and 0.26 pu, respectively. In each simulation the 5 mile simulation was capable of sustaining the load profile from the DWPT network. However, the load demand generated from the 10 mile and 15 mile scenarios drop significantly below the threshold between hour 9 and hour 22. This signifies

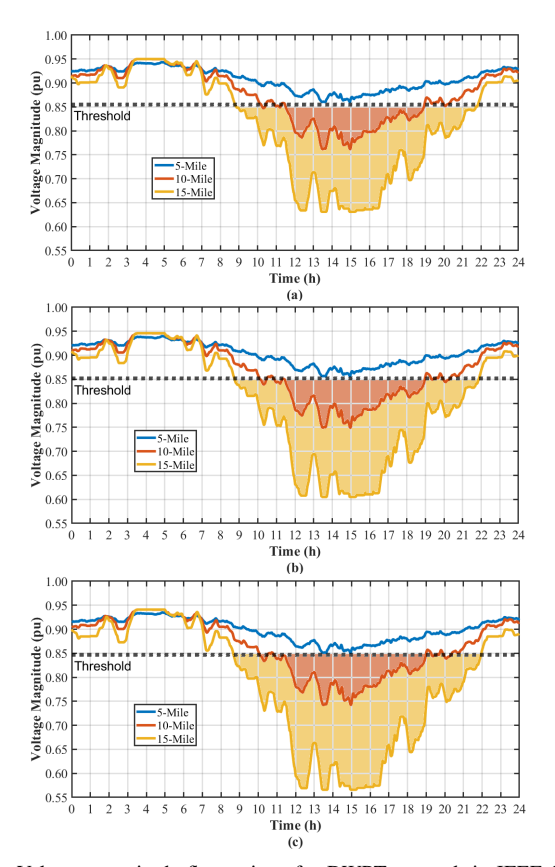


Fig. 8. Voltage magnitude fluctuations for DWPT network in IEEE 33-Bus distribution grid. (a) Bus-6, (b) Bus-7, and (c) Bus-8.

that the system would experience potential negative effects if mitigation strategies are not implemented to sustain the load. Otherwise, the load during this period would need to be shed to preserve grid stability, thus preventing EV users from charging during the most active periods of the day.

## C. Summary and Discussion of Results

The microscopic TF simulation for a two-lane highway demonstrates that the load demand from DWPT networks not only reduces based on randomized vehicle behaviors but also increases with the length of the charging system and TF totals. The obtained simulation results presented the behavior of each EV that traversed through the DWPT networks and was able to achieve the best average increase of SOC during the 15 mile DWPT network. However, the distribution grid simulations demonstrated that the 15 mile scenario would experience detrimental voltage fluctuations that would require additional planning and strategies (e.g., installing voltage support equipment or load mitigation) to prevent grid stability from reducing. Therefore, test results demonstrated that a IEEE 33-bus distribution grid would be capable of sustaining a 5 mile DWPT network with no additional planning or strategies to mitigate load demands or voltage fluctuations.

## V. CONCLUSION

This paper demonstrated the implementation of the proposed approach for a two-lane microscopic simulation of a DWPT network at various lengths. The simulation results provided a comprehensive overview of the proposed approach to generate a more accurate calculation of the behavior of each vehicle as well as the charging characteristics of EVs during each time interval. For all of the DWPT network lengths, i.e., 5 mile, 10 mile, and 15 mile, considered in this paper, the average SOC for all EVs increased significantly, thus proofing the feasibility of the charging system to provide adequate increases to the SOC of all users while the vehicle is in-motion. However, at the higher DWPT network lengths, the load demand generated from the EVs would result into negative effects on the distribution grid if mitigation strategies are not implemented properly.

Future work would be interesting to conduct a thorough analysis on the reliability of the DWPT networks for different distribution grid topology as well as to determine novel metrics for their implementation. This would benefit the planning and construction phases of DWPT networks to ensure that system operators of both electrical power grids and transportation networks can reliably implement these complex charging networks for sustainable and equitable power-transportation infrastructure.

#### REFERENCES

- S. Lukic and Z. Pantic, "Cutting the cord: Static and dynamic inductive wireless charging of electric vehicles," *IEEE Electrification Magazine*, vol. 1, no. 1, pp. 57–64, 2013.
- [2] U. D. of Energy. "Alternative fuels data center: Electric vehicle benefits and considerations." (2024), [Online]. Available: https://afdc. energy.gov/fuels/electricity\_benefits.html.

- [3] F. Turki, V. Staudt, and A. Steimel, "Dynamic wireless ev charging fed from railway grid: Magnetic topology comparison," in 2015 International Conference on Electrical Systems for Aircraft, Railway, Ship Propulsion and Road Vehicles (ESARS), 2015, pp. 1–8.
- [4] USAFacts. "How much electricity would it take to power all cars if they were electric?" (2024), [Online]. Available: https://usafacts.org/ articles/how-much-electricity-would-it-take-to-power-all-cars-ifthey-were-electric/.
- [5] S. Maji, D. Etta, and K. K. Afridi, "A high-power large air-gap multimhz dynamic capacitive wireless power transfer system utilizing an active variable reactance rectifier for ev charging," in 2022 IEEE Energy Conversion Congress and Exposition (ECCE), 2022, pp. 1–6.
- [6] R. M. Nimri, A. Kamineni, and R. Zane, "A modular pad design compatible with sae j2954 for dynamic inductive power transfer," in 2020 IEEE PELS Workshop on Emerging Technologies: Wireless Power Transfer (WoW), 2020, pp. 45–49.
- [7] A. Sagar, A. Kashyap, M. A. Nasab, S. Padmanaban, M. Bertoluzzo, A. Kumar, and F. Blaabjerg, "A comprehensive review of the recent development of wireless power transfer technologies for electric vehicle charging systems," *IEEE Access*, vol. 11, pp. 83703–83751, 2023.
- [8] J. Kracek and M. Svanda, "Analysis of capacitive wireless power transfer," *IEEE Access*, vol. 7, pp. 26678–26683, 2019.
- [9] A. Zakerian, S. Vaez-Zadeh, and A. Babaki, "A dynamic wpt system with high efficiency and high power factor for electric vehicles," *IEEE Transactions on Power Electronics*, vol. 35, no. 7, pp. 6732–6740, 2020.
- [10] S. Inoue, D. Goodrich, S. Saha, R. Nimri, A. Kamineni, N. S. Flann, and R. A. Zane, "Fast design optimization method utilizing a combination of artificial neural networks and genetic algorithms for dynamic inductive power transfer systems," *IEEE Open Journal of Power Electronics*, vol. 3, pp. 915–929, 2022.
- [11] B. J. Varghese, R. A. Zane, A. Kamineni, R. Tavakoli, Z. Pantic, C. Chou, and L. Liu, "Multi-pad receivers for high power dynamic wireless power transfer," in 2020 IEEE Energy Conversion Congress and Exposition (ECCE), 2020, pp. 5162–5168.
- [12] S. Liu, Y. Li, Y. Wu, L. Zhou, X. Zhao, R. Mai, and Z. He, "An output power fluctuation suppression method of dwpt systems based on dualreceiver coils and voltage doubler rectifier," *IEEE Transactions on Industrial Electronics*, vol. 70, no. 10, pp. 10167–10179, 2023.
- [13] L. Xue, V. Galigekere, G.-j. Su, R. Zeng, M. Mohammad, E. Gurpinar, S. Chowdhury, and O. Onar, "Design and analysis of a 200 kw dynamic wireless charging system for electric vehicles," in 2022 IEEE Applied Power Electronics Conference and Exposition (APEC), 2022.
- [14] T. Newbolt, P. Mandal, H. Wang, and R. Zane, "Load demand modeling of large-scale charging infrastructure for electric vehicles in-motion," *IEEE Access*, 2024, [under review].
- [15] M. said EL HMAM, H. ABOUAISSA, D. JOLLY, and A. BE-NASSER, "Macro-micro simulation of traffic flow," *IFAC Proceed*ings Volumes, vol. 39, no. 3, pp. 351–356, 2006.
- [16] I. I. of Technology Bombay. "Microscopic traffic simulation." (2024), [Online]. Available: https://www.civil.iitb.ac.in/~vmtom/nptel/ 535\_TrSim/web/web.html#:~:text=A%20microscopic%20model% 20of%20traffic,different%20features%20of%20a%20road.
- [17] T. Newbolt, P. Mandal, H. Wang, and R. Zane, "Sustainability of dynamic wireless power transfer roadway for in-motion electric vehicle charging," *IEEE Transactions on Transportation Electrification*, vol. 10, no. 1, pp. 1347–1362, 2024.
- [18] U. S. D. of Transportation. "United states traffic volume data." (2024), [Online]. Available: https://www.fhwa.dot.gov/policyinformation/tables/tmasdata/#y20.
- [19] E. V. Specifications. "Ev specifications news." (2023), [Online]. Available: https://www.evspecifications.com.
- [20] T. Newbolt, P. Mandal, H. Wang, and R. Zane, "Priority load control for dynamic wpt roadway in electrified transportation infrastructure," in *IEEE Power and Energy Society General Meeting (PESGM)*, 2023.
- [21] B. of Transportation Statistics. "Number of u.s. aircrafts vehicles vessels and other conveyances." (2023), [Online]. Available: https: //www.bts.gov/content/number-us-aircraft-vehicles-vessels-andother-conveyances.
- [22] "Ieee draft recommended practice for monitoring electric power quality," *IEEE P1159/D6, January 2019*, pp. 1–104, 2019.